REVIEW

Type IV cracking in ferritic power plant steels

J. A. Francis*[1], W. Mazur[2] and H. K. D. H. Bhadeshia[3]

There have been concerted world wide efforts to develop steels suitable for use in efficient fossil fired power plants. Ferritic alloys containing between 9 and 12 wt-% chromium are seen as the most promising materials in this respect, especially for thick walled components such as headers and the main steam pipe in boilers. However, the performance of the improved steels has often not been realised in service, because premature failures occur in the heat affected zone of welded joints in a phenomenon referred to as type IV cracking. This review assesses the relationship between the composition and microstructure of 9–12 Cr steels, the welding and fabrication procedures and how these factors translate into a propensity for type IV failures.

Keywords: Creep, Steel, Heat affected zone, Power plant, Type IV, Weld

Introduction

The prospect of global warming has stimulated the search for strategies which lead to a reduction in CO_2 emissions. The energy sector is a major CO_2 producer and hence has been the subject of particular scrutiny. In the European Union, for example, $\sim$50% of electricity production in the year 2000 was derived from the burning of fossil fuels.[1]

Fossil fired power plants rely on steam turbines to generate electricity. Their thermodynamic efficiency can be increased if the temperature and pressure of the steam entering the turbines is increased.[2] This is the reason for the intense efforts throughout the world to develop steels capable of sustaining the harsher conditions necessary for efficient power generation.[1,3,4] The National Institute for Materials Science in Japan, for example, has a long term objective of developing steels for ultra supercritical power plants operating with steam conditions of 650°C at a pressure of 35 MPa,[5] and there are similar efforts encouraged by the European Union.

Ferritic creep resistant steels containing up to 2·25 wt-% chromium and 1 wt-% molybdenum have been available since the 1940s.[6] They are capable of supporting 40 MPa of stress at 560°C.[7] In contrast, the more expensive 304 austenitic stainless steel can cope with 40 MPa at the substantially higher service temperature of 650°C. However, austenitic steels suffer from a much higher thermal expansivity and lower thermal conductivity, making them susceptible to thermal fatigue, particularly in thick sections and in operating conditions involving frequent shut-downs and variable power demands.[1,7] The focus of research is therefore ferritic steels, at least as far as the goal of a 650°C steam temperature is concerned.[6]

This goal has as yet proved impossible to achieve. Alloys such as NF616 (9Cr–0·5Mo–1·8WVNb) and HCM12A (11Cr–0·4Mo–2W–CuVNb) are currently being tested for service at 625°C.[8] But there are problems of premature failure at welded joints, particularly in the heat affected zone (HAZ) of the welds.[5,6] The cracking of welded joints is usually classified according to the position of the crack. Type I and type II modes occur within the weld metal, the former confined to the weld metal whereas the latter may grow out of the weld into the plate. Type III cracking occurs in the coarse grained region of the HAZ. Type IV is a pernicious form of cracking where there is an enhanced rate of creep void formation in the fine grained and intercritically annealed HAZ of the weld, leading to early failure when compared with creep tests on the unwelded steel.

The purpose of this article is to review progress in understanding and mitigating type IV failures in ferritic power plant steels, including the relationship between the composition and microstructure of susceptible steels, the welding and fabrication procedures and how these factors translate into a propensity for type IV failures. Methods of weld repair for existing creep damage have been reviewed elsewhere.[9] The focus here is on the newer steels containing between 8·5 and 12 wt-% chromium, i.e., candidate materials for future power plant applications.[4] We begin with a description of the steel metallurgy, followed by that of the welded structure, in the context of type IV cracking.

Steels

The development of 9Cr steels with higher temperature capabilities than the classical 2·25Cr–1Mo grades has been described elsewhere[6,7,10,11] but a summary is relevant here to set the scene for type IV creep failures. The first high chromium ferritic steels appeared in Europe in the mid 1960s. A 9Cr–2Mo steel was developed in France primarily for tubing and subsequently named

[1]Research Fellow, School of Materials, University of Manchester, Grosvenor Street, Manchester, M1 7HS, UK
[2]CSIRO Manufacturing and Infrastructure Technology, Woodville, SA 5011, Australia
[3]Department of Materials Science and Metallurgy, University of Cambridge, Pembroke Street, Cambridge CB2 3QZ, UK

*Corresponding author, email John.Francis@manchester.ac.uk

Published by Maney on behalf of the Institute
Received 29 March 2006; accepted 12 May 2006
DOI 10.1179/174328406X148778

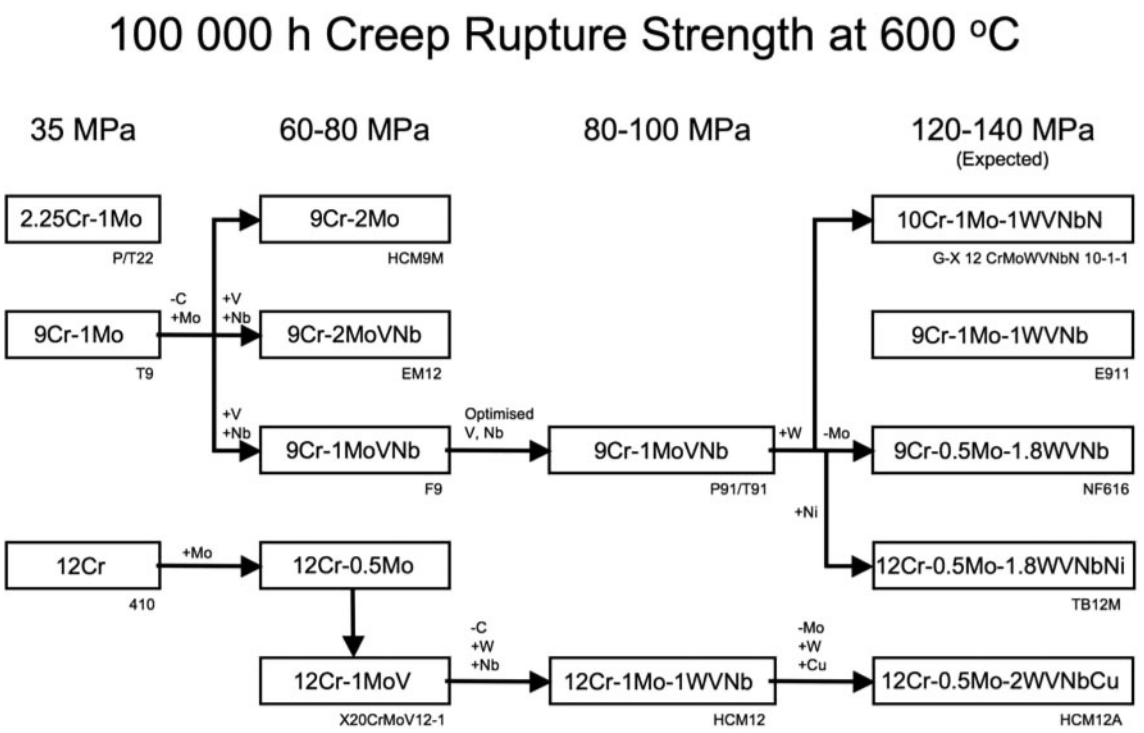

1 Evolution of 9–12 Cr ferritic heat resistant steels[17]

EM12. This had a duplex microstructure containing δ-ferrite, giving poor impact toughness.[6] At about the same time a 12Cr–1Mo steel was developed in Germany with the designation X20CrMoV12–1 and applied throughout the world for tubes and pipes. While this steel benefited from a fully martensitic microstructure, it exhibited inferior creep strength to EM12 at temperatures $>520^{\circ}$C and was difficult to weld, primarily owing to a high carbon content.[6]

In the 1970s the Oak Ridge National Laboratory (USA) developed a modified 9Cr–1Mo steel,[12] leading ultimately to T91 for pressure tube applications and alloy P91 for piping and headers; this superseded EM12 and X20CrMoV12–1. The alloy relies on a tempered martensitic microstructure stabilised by $M_{23}C_6$ carbides, with further strengthening owing to molybdenum in solid solution and a fine distribution of vanadium/niobium rich carbonitride (MX) precipitates.[10]

Reliable further improvements in creep strength have been achieved with the advent of steels such as NF616 and HCM12A, where tungsten enhances the long term creep strength through solid solution hardening[13] and retards the coarsening of $M_{23}C_6$ carbides (which stabilise the martensite lath structure).[14] However, at concentrations in excess of 2 wt-%, the formation of coarse laves phase (Fe_2W) can lead to a deterioration of creep properties.[15] Tungsten also promotes the formation of δ-ferrite, so its use has to be balanced, either by reductions in the concentrations of other ferrite promoting solutes such as molybdenum, or by adding austenite stabilisers such as cobalt.[16] The evolution of the 9–12 Cr ferritic steels is illustrated in Fig. 1.[17] Table 1 lists the chemical compositions for various steels.[6] It can be seen that many of the modern steels contain tungsten in the range 1–2 wt-%.

Many of the new alloys which exhibited improved creep rupture strength in short term tests have disappointed when 100 000 h data became available. As a result, the focus of research has shifted to understanding the factors that affect the long term stability of $M_{23}C_6$ and MX precipitates. In creep tested steels a 'modified Z-phase', Cr(V,Nb)N (Ref. 18) seems to precipitate at the expense of $M_{23}C_6$ and vitally, the MX precipitates.[16,20] Recent studies have examined the effect of

Table 1 Typical chemical compositions for various steels.[6]

	Typical chemical composition, wt-%										
Steels	C	N	Si	Mn	Cr	Mo	V	Nb	W	Co	Cu
ASME P/T22	0·12	–	0·3	0·45	2·25	1·0	–	–	–	–	–
ASME T9	0·12	–	0·6	0·45	9·0	1·0	–	–	–	–	–
HCM9M	0·07	–	0·3	0·45	9·0	2·0	–	–	–	–	–
EM12	0·10	–	0·4	0·10	9·0	2·0	0·30	0·40	–	–	–
X20CrMoV-12-1	0·20	–	0·4	0·60	12·0	1·0	0·25	–	–	–	–
ASME P/T91	0·10	0·05	0·4	0·45	9·0	1·0	0·20	0·08	–	–	–
HCM12	0·10	0·03	0·3	0·55	12·0	1·0	0·25	0·05	1·0	–	–
GX12CrMoWVNbN-10-1-1	0·13	0·05	0·3	0·60	10·5	1·0	0·23	0·08	1·0	–	–
NF616 (ASME P/T92)	0·07	0·06	0·1	0·45	9·0	0·5	0·20	0·05	1·8	–	–
HCM12A (ASME P/T122)	0·11	0·06	0·1	0·60	12·0	0·4	0·20	0·05	2·0	–	1·0
SAVE12	0·10	0·04	0·3	0·20	11·0	–	0·20	0·07	3·0	3·0	–

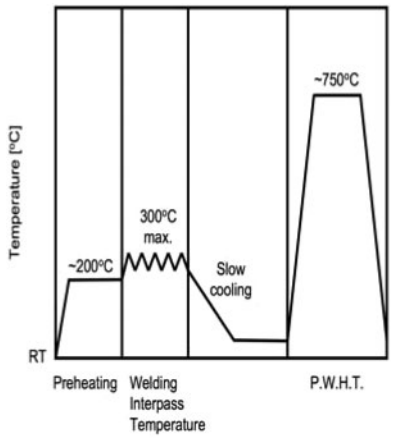

PWHT: post-weld heat treatment; RT: room temperature[10]

2 Typical temperature schedules for welded joints in P91 steel

carbon concentration and controlled additions of boron on the $M_{23}C_6$ and MX precipitation behaviour.[21,22]

Welding procedures

Ferritic 9–12 Cr power plant steels are generally supplied in a normalised and tempered condition. Tempering is recommended following welding, to reproduce as far as is possible, a tempered martensitic microstructure and to relieve some of the stresses induced by welding. The workpiece is frequently preheated to avoid cold cracking, followed by natural cooling to ambient temperature which is slightly below the martensite finish temperature.[10,11] A typical temperature schedule for a welded joint in P91 steel is presented in Fig. 2.[10]

Figure 3 represents a cross-section through a welded joint in a thick walled 9–12 Cr ferritic steel pipe. Given its ability to make high quality welds, gas tungsten arc welding (GTAW) is often used to complete the root pass which, because it is the first physical joint between the component plates, is particularly vulnerable to contraction strains. The same process can be used to complete the joint but manual metal arc welding (MMAW) is often used in complex joints, or high productivity processes such as flux cored arc welding (FCAW) and submerged arc welding for deep welds. The choice of process may also depend on whether the pipe is to be welded in a workshop or in situ. Alternatives to arc welding such as electron beam welding can also be employed.[23]

Filler metals for welding the 9–12 Cr steels are required to match the creep strength of the parent material in service. Ideally they would also have matching toughness at ambient temperatures, since welded joints are exposed to transient stresses during shut down periods. However, in early development work it became apparent that it would not be possible for weld metals to simultaneously meet both requirements.[10,11] As such, commercial filler metals tend to have a similar composition to the parent material, with matching creep strength but lower toughness. There is a tendency to include higher levels of manganese (0·6–0·7 wt-%) and nickel (0·4–0·6 wt-%) in order to improve weld metal toughness.[24] Gas tungsten arc welding consumables are

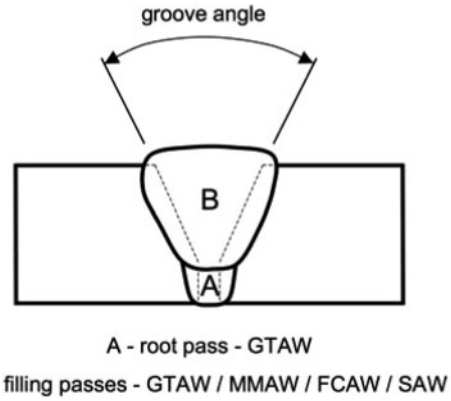

3 Schematic representation of welded joint in 9–12 Cr ferritic steel[10]

thought to achieve higher toughness than those for MMAW and FCAW, possibly owing to lower oxygen contents in the weld metal.[25]

In the context of type IV phenomena, there is little information on the effects of heat input and preheat temperature on the subsequent creep performance of welded joints. The choice of preheat temperature is aimed solely at the avoidance of cracking on cooling after welding.[10,11] It is also useful to deposit multiple beads to improve the toughness of welds. It has been reported that a narrow HAZ is conducive to enhanced creep performance and that reducing the groove angle in the joint preparation (Fig. 3) can improve creep life.[23,26] These conclusions hold for creep durations $<10\,000$ h, but further testing at lower stresses is required to establish whether the benefits are maintained over more realistic time periods.

Albert *et al.*[27,28] investigated the effect of the duration of post weld heat treatment on the creep performance of welded joints in an 11Cr–0·5Mo–2WCuVNb steel. Their samples were extracted from a gas tungsten arc weld in a 27 mm thick plate and subsequently tested at 70 MPa and 650°C. All specimens were post-weld heat treated at 740°C, for between 15 and 260 min. No significant effect of treatment time was noticed over this range, although those samples treated for longer than 60 min performed slightly better.

Detail within HAZ

Type IV failures occur because of the gradients of microstructure in the HAZ of welds. The microstructural regions that arise are illustrated in Fig. 4 and have been categorised by Mannan and Laha[29] as follows:

(i) coarse grain region (CGHAZ): Material near the fusion boundary that reaches a temperature well above Ac_3 during welding. Any carbides, which constitute the main obstacle to growth of the austenite grains, dissolve resulting in coarse grains of austenite. In the 9–12 Cr steels, this austenite transforms into martensite on cooling

(ii) fine grain region (FGHAZ): Away from the fusion boundary where the peak temperature T_P is lower, but still above Ac_3. Austenite grain growth is limited by the incomplete dissolution of carbides. Fine grained austenite is produced, which subsequently transforms into martensite in the 9–12 Cr steels

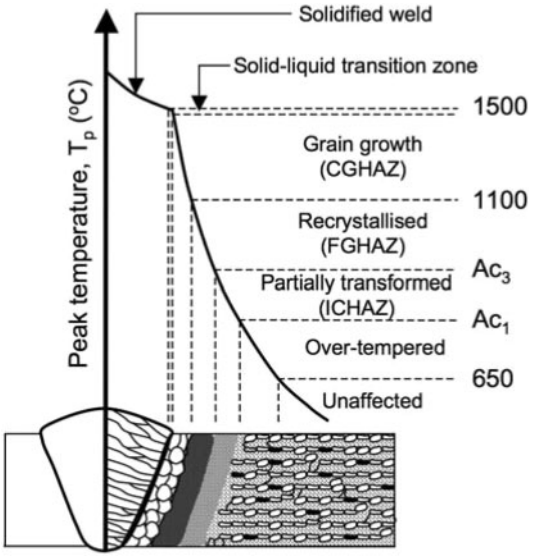

4 Schematic representation of microstructures developed in HAZ as approximate function of peak temperature during welding[29] Type IV failures are localised to the FGHAZ region, adjacent to the ICHAZ

(iii) intercritical region (ICHAZ): Here $Ac_1 < T_P < Ac_3$, resulting in partial reversion to austenite on heating. The new austenite nucleates at the prior austenite grain boundaries and martensite lath boundaries, whereas the remainder of the microstructure is simply tempered. The austenite (in 9–12 Cr steels) transforms into untempered martensite on cooling

(iv) over tempered region: With T_P below Ac_1 the original microstructure of the plate material undergoes further tempering.

Post-weld heat treatment tempers any virgin martensite introduced by the welding thermal cycles, but gradients in the microstructure and mechanical properties, extending typically over a few millimetres from the fusion surface, persist even after this treatment. The mechanical properties of individual zones can in principle be studied by subjecting bigger steel samples to the expected thermal cycle, in order to produce a homogeneous microstructure typical of one of the subzones described above.

Creep tests on HAZ simulated specimens for an 11Cr–0·4Mo–2WVNbCu (P122) steel with Ac_1 and Ac_3 at 820 and 920°C respectively, were carried out by Albert *et al.*[30] Simulated HAZ zones representative of GTAW were created using two techniques: furnace treatment and a Gleeble simulator. The simulated samples were 'post-weld' treated at 740°C before creep testing. The results are illustrated in Fig. 5. The lowest rupture time at a given stress corresponds samples subjected to T_P at or just above Ac_3 (equivalent to FGHAZ). The two simulation methods produced comparable results except for the highest values of T_P. Unlike a furnace, a weld simulator heats the sample locally with a uniform temperature zone of ~15 mm over a sample length of 120 mm. Furthermore, samples heated to temperatures higher than Ac_3 tended to rupture outside the uniform temperature zone, in a location with a microstructure corresponding to T_P just above Ac_3. Furnace heat treatments therefore give more reliable simulated samples.

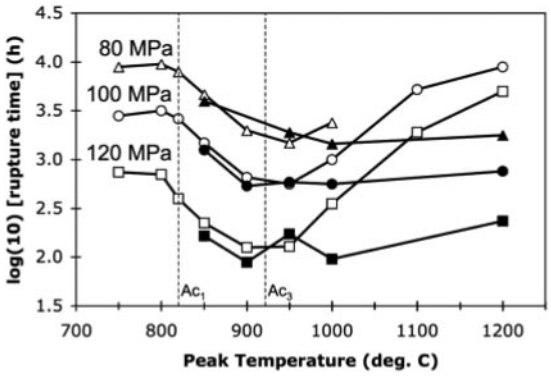

open points: furnace heat treatment; closed points: weld simulator

5 Rupture times for HAZ simulation coupons in ASME-P122 steel[30]

Tabuchi, Abe and co-workers also studied the P122 HAZ using furnace simulated samples (Fig. 6).[3,31] At all stress levels, the minimum creep life was observed for T_P at or just above Ac_3 (920°C (Ref. 30)). The minimum hardness before creep testing occurred at T_P=850°C (ICHAZ in P122), as shown in Fig. 6. There was evidence that the minimum creep life and minimum hardness occurred in the same region of the HAZ at high stresses, although the rupture location changed to a greater T_P when the stress was reduced towards service levels. In the latter case, the location corresponding to minimum hardness clearly is not useful in identifying the location of creep failure.

Type IV failures

A limited number of uniaxial, cross-weld creep tests have been openly reported for 9–12 Cr steels[3,4,8,26,27,32–34] together with a few longitudinal tests on seam welded pipe sections subjected to internal pressure.[4] In the latter case the highest principal stress is transverse to the welding direction and the test is not uniaxial.

In a cross-weld test the sample fails in either the weld metal, HAZ or parent material. For 9–12 Cr steels, the creep strength of the weld metal usually at least matches that of the parent material, so failures generally occur either in the parent material or HAZ.[10,11] Recently, an analysis was carried out of published data relating to cross-weld creep tests on several different 9–12 Cr steels.[35] Based on the results of 53 tests, it was noted that

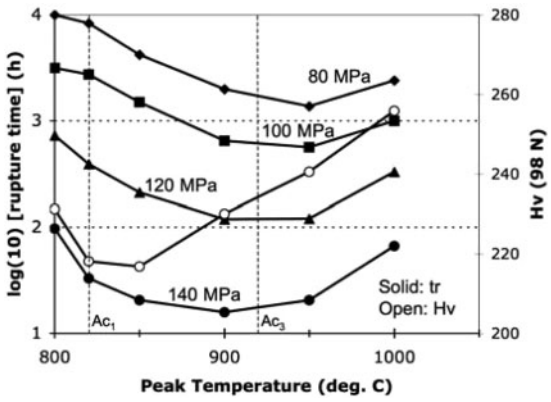

6 Rupture times for furnace heat treated HAZ simulation coupons in ASME-P122 steel[3]

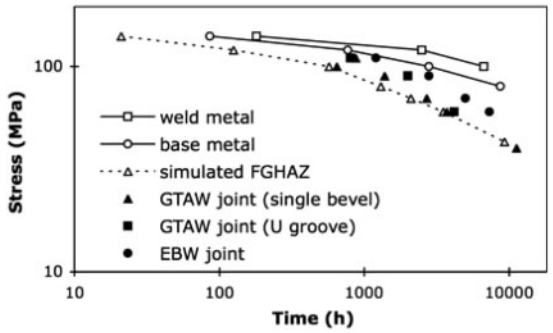

7 Type IV rupture data for welded joints in ASME-P122 steel at 650°C (Ref. 3)

type IV failures predominate when the applied stress is less than 100 MPa. The shift in fracture location from the base material to the HAZ is both stress and temperature dependent, with stress being the more important influence.[10,11] At least one tube and pipe manufacturer refers to a critical stress, ~120 MPa, below which weldments are expected to be limited by type IV failure.[10,11]

The relationship between stress and the tendency for type IV failure is nicely illustrated in data presented by Abe and Tabuchi,[3] who compared weld metal, base metal and the simulated FGHAZ against cross-weld rupture data for joints in P122 steel. Welds were made with electron beam welding, as well as with the gas tungsten arc process, using two different joint preparations. It is evident in Fig. 7 that the creep strength of the weld metal exceeds that of the base metal and that the worst performance is of the simulated FGHAZ specimens. All of the joints failed in the type IV region, i.e. the fine grained HAZ region adjacent to the intercritical HAZ. The rupture times for the joints were between those of the base metal and simulated FGHAZ. At stresses just above 100 MPa, the creep performance of welds approaches that of the base metal. However, as the test stress is reduced the difference between the rupture lives of the welds and the base metal increases, until at low stresses the rupture lives for welds approach those for the simulated FGHAZ.

The data in Fig. 7 show some systematic differences in the creep lives of welded joints, which indicate that the welding process and joint configuration must influence life, especially for high stresses. The influence of welding parameters on type IV failure has been investigated using a Bayesian neural network analysis of data obtained from 53 well characterised cross-weld experiments.[36] The input variables consisted of the chemical composition (including the 9–12 Cr alloys), details of the initial heat treatment of the steel, welding parameters, post weld heat treatment, test temperature and rupture time. The output was the rupture stress.

The abilities of a variety of variables in explaining the observed changes in type IV rupture stress (the significance of each input) are shown in Fig. 8.[36] A large value of the significance means that the particular variable is important in determining the rupture stress in the context of the data examined. The time to rupture and test temperature obviously greatly influence the stress but some well known effects of normalising temperature,[37] tempering and the strong effect of tungsten[6] are clearly evident. Given that the model is

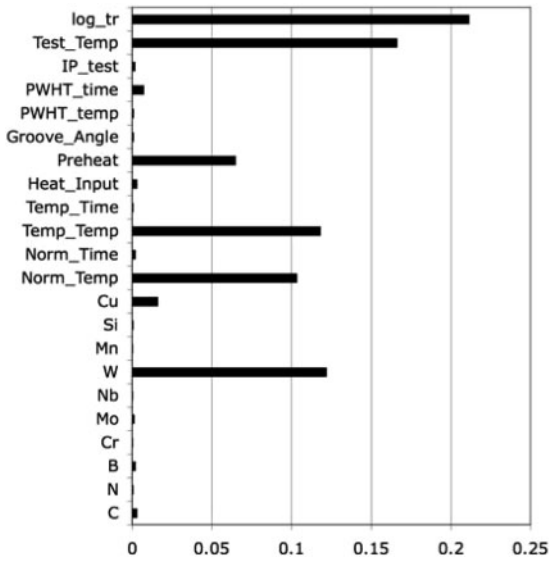

8 Perceived significance of type IV rupture stress to a variety of parameters[36]

well behaved, it gives confidence in the interpretation of the importance of the other parameters. There are clear indications that an increase in the preheat temperature could be important in enhancing the rupture stress. The heat input is perceived to be insignificant, which is useful when high productivity welding is required. These predictions have yet to be verified systematically.

Microstructural evolution

The 9–12 Cr alloys are supplied in a tempered martensitic condition; the finely dispersed lath boundaries, pinned typically by $M_{23}C_6$ carbides,[10,11] are good for retarding creep. Further strengthening relies on solid solution strengthening from solutes such as molybdenum and tungsten and fine distributions of V/Nb carbonitrides (MX) which are seminal in ensuring very long term creep properties.[38] The microstructure evolves during elevated temperature service, with general coarsening and the further precipitation of more stable and rather coarse phases such as laves and Z-phase.[18] This depletes solid solution strengthening solutes and at the same time causes the dissolution of MX particles, leading to a dramatic deterioration in creep properties.[38] Coarse particles also stimulate the nucleation of voids during the latter stages of creep.[30,39]

The coarsening has been characterised quantitatively; Hofer *et al.*[40] studied a cast martensitic steel (GX12CrMoWVNbN-10-1-1), after aging for periods of up to 33 410 h at 600°C (Fig. 9). Only $M_{23}C_6$ carbides and vanadium nitride were detected in the as received condition (Fig. 9*a*). Laves phase and niobium carbonitrides appeared after aging for 976 h (Fig. 9*b*). Once present, laves phase was observed to coarsen rapidly (Fig. 9*c* and *d*) and Z-phase appeared (at the expense of MX) after aging for 33 410 h. The results suggest that laves phase, because it coarsens rapidly, is likely to promote the onset of tertiary creep over the long term.[41] In contrast, the stability of $M_{23}C_6$ and MX is critical to the long term performance of these alloys.

The effects of welding thermal cycles on the carbide dispersions and creep strength in a 10Cr–3W–3CoVNb steel (SAVE12 in Table 1) have been investigated by

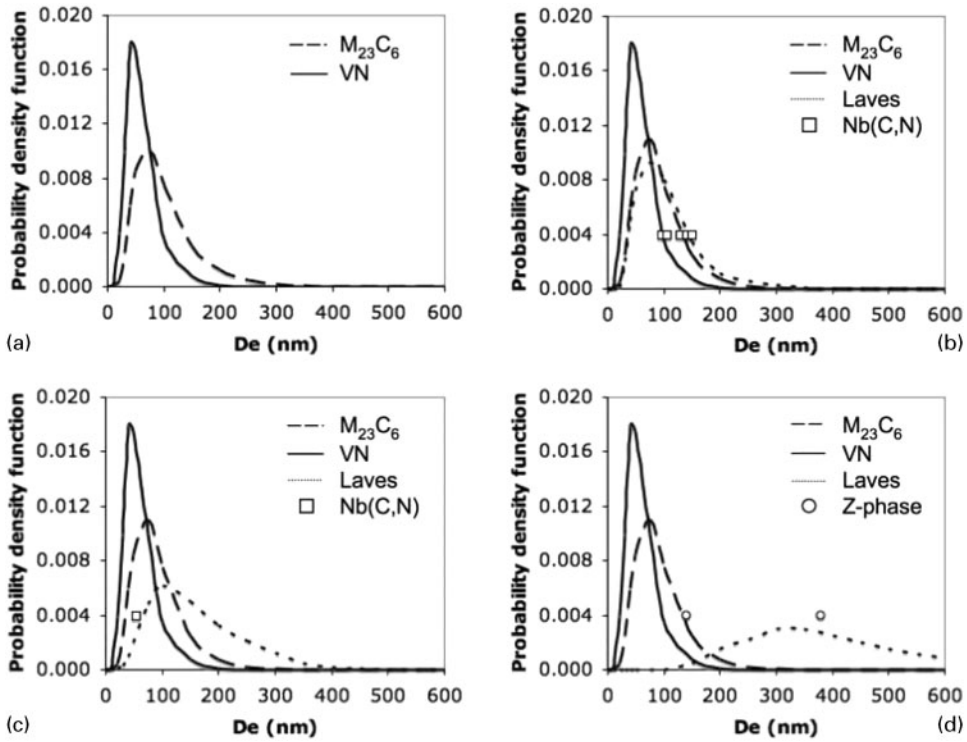

9 Distributions of precipitates in X12CrMoWVNbN-10-1-1 steel in terms of an equivalent diameter D_e in *a* as received condition, *b* 600°C/976 h, *c* 600°C/5 014 h and *d* 600°C/33 410 h (Ref. 40)

Hirata and Ogawa.[42,43] They used induction heated HAZ simulated specimens with T_P in the range 830 to 1200°C, subjecting them to creep at 650°C with a stress of 98 MPa. The precipitates in the over tempered regions did not dissolve as a consequence of the weld thermal cycle with T_P=830°C, just above Ac_1. In the coarse grained HAZ with T_P=1200°C, the precipitates almost completely dissolved but were reprecipitated during the post-weld heat treatment. In the fine grained HAZ with T_P=1000°C (just above Ac_3), carbides containing chromium or vanadium underwent partial dissolution with reprecipitation and relatively rapid coarsening during the post-weld heat treatment and subsequent creep, far more so than in the other zones. After 5014 h there were indications of Z-phase in the fine grained HAZ, a phase associated with reduced creep properties.[16,20,40]

These observations are important because the partial dissolution of $M_{23}C_6$ in the fine grained HAZ promotes Z-phase which in turn destabilises MX. The resulting deterioration of creep thus becomes localised to the type IV region.

Some fascinating results have recently been reported on the influence of boron on type IV failure in 9–12 Cr steels.[22,44] Albert *et al.*[22] found that such failures were suppressed in a 9Cr–3W–3CoVNb steel containing boron in the range 90–130 ppm, with nitrogen kept <0·002 wt-%. At stresses >100 MPa, fracture occurred in the parent material, while for lower stresses the failure occurred at the fusion surface rather than in the usual type IV region, which is the HAZ heated to near Ac_3. There were reportedly no creep voids in the HAZ of fractured specimens. Curiously, the austenite grains remained large at a distance 1–2 mm from the fusion surface, the region where fine grained austenite is usually observed in the HAZ of welded joints. The reasons for this unusual HAZ microstructure have not been fully clarified, but it is suggested[22] that the low nitrogen content reduces the content of MX, thus allowing the austenite grains to coarsen, eliminating the FGHAZ which is weak in creep. In any event, none of the welds studied exhibited type IV cracking, with fracture occurring at the weld interface with rupture times comparable to that of the parent metal. This is a system which deserves further attention.

The mechanism of the boron effect is not clear; could it be that it influences austenite formation even at such minute concentrations? Much may be attributable to the absence of a fine grained HAZ, but it is also known that additions of boron have led to improved creep performance for the parent material, through the delayed coarsening of $M_{23}C_6$ carbides and a corresponding delay in the onset of tertiary creep.[22]

Stress evolution

Watanabe *et al.*[45] studied thermally aged 2·25Cr–1Mo, with and without an applied stress and found that coarsening was accelerated in the presence of stress. It is expected therefore that residual stresses resulting from welding are detrimental to creep properties, especially since coarse particles enhance the formation of voids.[30,39]

Although there are no specific data on residual stresses in 9–12 Cr steel weldments, the existence of such stresses is well established in general.[46–48]

Yaghi *et al.*[49] recently made numerical predictions for the residual stresses that arise in P91 circumferential pipe welds. Their results suggest that the location of the peak tensile residual stresses will vary with the wall thickness. Nevertheless, as the wall thickness becomes large, they consistently predict peak tensile residual stresses between 400 and 500 MPa near the outer surface

of the pipe; a result that becomes insensitive to further increases in wall thickness. There is a pressing need to validate such numerical predictions with experimental data. Furthermore, studies specific to the power plant steels would be useful in assessing the importance of parameters such as the preheat and post-weld heat treatment in determining residual stress distributions and the tendency for type IV cracking.

Because of the gradients of microstructure in the HAZ, there are corresponding gradients in the creep properties. If the creep resistance reaches a minimum at some location then complex constraint effects are expected during cross-weld loading, which may intensify local damage. Using a two-dimensional finite element technique, Li *et al.*[50] simulated creep in a P122 weldment by compiling a model consisting of four regions with different creep properties (weld metal, CGHAZ, FGHAZ and base metal). During creep, each zone within the weldment was assumed to obey Norton's creep law. The stress and strain distributions following 1000 h of creep at 90 MPa and 650°C were thus estimated. It was found that a high tensile first principal stress and high tensile hydrostatic stress were generated in the FGHAZ. It was argued that the strain focuses in the weaker FGHAZ during the early stages of creep, leading to the nucleation of creep voids, which are then encouraged to grow by the strain mismatch and triaxial stresses generated as creep progresses.

The triaxial stress state in the FGHAZ has been previously recognised to accelerate the growth of creep voids,[28,50] but this may not necessarily lead to a reduction in creep life. To illustrate this point, it is worth considering the data in Fig. 7, for P122 steel. Above 100 MPa, the creep performance of weldments is close to that for the parent material. Furthermore, as the applied stress is reduced, the creep performance of the weldments approaches (but still exceeds) that of the weakest zone within the weldment, i.e. the FGHAZ. If it is assumed that the triaxial stress states that arise in the FGHAZ accelerate the formation of creep voids, then it is intriguing that the creep lives of the welded joints, which failed owing to type IV cracking, were still longer than those for the simulated FGHAZ specimens (these, after all, are mechanically homogeneous and will not contain triaxial stresses). The data of Fig. 7 suggest that the mechanical constraint resulting from the property gradients in the HAZ actually delays failure in the FGHAZ.

An alternative approach to modelling type IV damage is due to Kimmins and Smith,[51] who used finite element representations of Cr–Mo weldments, allowing for the relaxation of constraint by the sliding of adjacent elements during creep. It is known that models based on transverse strain compatibility give rise to significant constraint of creep deformation in the weak zone.[52] However, it was pointed out that at lower service stresses grain boundaries are less resistant to sliding.[53] Thus, in contrast to continuum models where damage accumulation is enhanced by multiaxial stresses, Kimmins and Smith suggested that constraint is relaxed by grain boundary sliding.[51] They later presented evidence to suggest that grain boundary sliding in cross-weld specimens gives rise to greater numbers of cavities, consistent with their observation that greater numbers of cavities are observed in welded joints than in HAZ simulated specimens.[53] Finally, they noted that once sliding was accommodated and constraint relaxed, the failure time for both cross-weld specimens and simulated type IV specimens was similar.

Suggestions for future work

As a result of this assessment of literature, we believe that the following areas need particular attention in future research:

(i) Controlled additions of boron: Evidence clearly suggests type IV cracking can be suppressed using controlled additions of boron to 9–12 Cr steels. Concentrations between 90 and 130 ppm result in the elimination of the conventional fine grained HAZ; they stabilise $M_{23}C_6$ carbides, apparently through the partial substitution of carbon by boron. However, it is not clear which of these factors is responsible for the suppression of type IV failures, nor why it might be counterproductive to exceed a boron level of 130 ppm.

(ii) The stability of MX precipitates: MX precipitates are vital in determining the long term creep strength for 9–12 Cr steels. However, there are indications that the thermal cycles that are experienced in the fine grained HAZ promote a chromium-rich 'modified Z-phase' of the form Cr(V,Nb)N during creep at the expense of MX precipitates. Further work is required to establish how the fine grained HAZ is particularly susceptible to this deleterious phase and whether its formation can be avoided.

(iii) Significance of welding parameters: There is a dearth of studies relating welding parameters, particularly the preheat temperature and heat input, to the tendency for type IV cracking.

(iv) Role of stress: The role of residual stresses arising from welding, on the creep performance of 9–12 Cr steels, needs to be investigated with respect to their effect on the evolution of microstructure in the HAZ. Further work is also necessary to clarify the extent to which grain-boundary sliding is responsible for the formation of creep voids in longer-term creep tests. In general, greater emphasis needs to be placed on tests carried out at stresses below 100 MPa, as it is at these lower stress levels that type IV failures predominate.

Mechanism for type IV cracking

The focus on type IV cracking has in this review been on the 9–12Cr steels which are leading the search for steels useful in making ever more efficient power plants. For these steels, it appears that the microstructure which is weakest in creep is that associated with the FGHAZ of a weld. This is the zone which reaches temperatures just inside the austenite phase field, but not for long enough to allow carbide precipitates to completely dissolve. As a result, the austenite grains that form remain relatively fine and transform to martensite on cooling. On post-weld heat treatment, the undissolved carbides coarsen with limited further precipitation.

The FGHAZ does not correspond to the heat affected region with the lowest hardness, which is the zone that is

only partially austenitised (ICHAZ) and hence contains over tempered martensite.

At high stresses, using simulated samples with homogeneous microstructures, the minimum creep strength microstructure coincides with the minimum hardness microstructure (ICHAZ). However, at the low stresses typical of service conditions, the creep life is a minimum in the FGHAZ, which does not have the minimum hardness. This means that hardness cannot be used as an indicator of type IV susceptibility or type IV location.

The tests done on simulated samples containing homogeneous microstructures are revealing, but type IV cracking occurs in the FGHAZ of cross-weld specimens where the microstructure is far from uniform. Finite element simulations which treat the cross-weld test as a longitudinal series of different microstructures with different constitutive behaviours, predict triaxial stresses in the FGHAZ, which should accelerate the formation of creep voids. Taken at face value, this is odd because experiments with cross-weld samples show a greater resistance to creep than simulated FGHAZ samples. This is in spite of the fact that triaxial stresses will only be present in the FGHAZ of cross-weld samples.

The most reasonable explanation comes from the work of Kimmins and Smith, who allowed grain boundary sliding in their finite element models of the cross-weld scenario. They found that the constraint originating from the heterogeneous microstructure is relaxed by grain boundary sliding, making failure easier in the FGHAZ. This is consistent with the poor creep properties of a simulated, homogeneous FGHAZ.

These results lead to a simple conclusion, that anything carried out to strengthen grain boundaries, for example the addition of boron, may allow constraint to appear in a cross-weld test, thereby increasing the life for type IV fracture.

Acknowledgements

This work was undertaken as part of a project that is proudly supported by the International Science Linkages programme established under the Australian Government's innovation statement Backing Australia's Ability.

References

1. H. Cerjak: Proc. Int. Conf. on 'Achievements and perspectives in producing welded construction for urban environments', 56th IIW Annual Assembly, Bucharest, Romania, July 2003, ASR, 15–24.
2. H. K. D. H. Bhadeshia: *ISIJ Int.*, 2001, **41**, (6), 626–640.
3. F. Abe and M. Tabuchi: *Sci. Technol. Weld. Join.*, 2004, **9**, (1), 22–30.
4. K. Shinozaki, D. Li, H. Kuroki, H. Harada, K. Ohishi and T. Sato: *Sci. Technol. Weld. Join.*, 2003, **8**, (4), 289–295.
5. M. Tabuchi, T. Watanabe, K. Kubo, M. Matsui, J. Kinugawa and F. Abe: *Int. J. Press. Vess. Pip.*, 2001, **78**, 779–784.
6. C. D. Lundin, P. Liu and Y. Cui: 'A literature review on characteristics of high temperature ferritic Cr–Mo steels and weldments', WRC bulletin 454, Welding Research Council, Inc., New York, NY, USA, 2000.
7. 'Metals handbook', 10th edn, Vol. 1, 'Elevated temperature properties of ferritic steels', 617–652; 1990, Materials Park, OH, ASM International.
8. M. Matsui, M. Tabuchi, T. Watanabe, K. Kubo, J. Kinugawa and F. Abe: *ISIJ Int.*, 2001, **41**, S126–S130.
9. S. Issler, A. Klenk, A. A. Shibli and J. A. Williams: *Int. Mater. Rev.*, 2004, **49**, (5), 299–324.
10. K. Haarmann, J. C. Vaillant, B. Vandenberghe, W. Bendick and A. Arbab: 'The T91/P91 book'; 2002, Boulogne, Vallourec & Mannesmann Tubes.
11. D. Richardot, J. C. Vaillant, A. Arbab and W. Bendick: 'The T92/P92 book'; 2000, Boulogne, Vallourec & Mannesmann Tubes.
12. V. K. Sikka and P. Patriarca: 'Analysis of weldment mechanical properties of modified 9Cr–1Mo steel', Technical report, Metals and Ceramics Division, Oak Ridge National Laboratory, Oak Ridge, TN, USA, 1984.
13. K. Iwanaga, T. Tsuchiyama and S. Takaki: *Key Eng. Mater.*, 2000, **171–174**, 477–482.
14. F. Abe: *Key Eng. Mater.*, 2000, **171–174**, 395–402.
15. Y. Hasegawa, T. Muraki, M. Ohgami and H. Mimura: *Key Eng. Mater.*, 2000, **171–174**, 427–436.
16. C. Berger, A. Scholz, Y. Wang and K. H. Mayer: *Z. Metallkd*, 2005, **96**, (6), 668–674.
17. H. Cerjak and E. Letofsky: *Sci. Technol. Weld. Join.*, 1996, **1**, (1), 36–42.
18. A. Strang and V. Vodarek: *Mater. Sci. Technol.*, 1996, **12**, (7), 552–556.
19. I. L. Papst, P. Warbichler, F. Hofer, E. Letofsky and H. Cerjak: *Z. Metallkd*, 2004, **95**, (1), 18–21.
20. E. Letofsky and H. Cerjak: *Sci. Technol. Weld. Join.*, 2004, **9**, (1), 31–36.
21. M. Taneike, K. Sawada and F. Abe: *Metall. Mater. Trans. A*, 2004, **35A**, (4), 1255–1262.
22. S. K. Albert, M. Kondo, M. Tabuchi, F. Yin, K. Sawada and F. Abe: *Metall. Mater. Trans. A*, 2005, **36A**, (2), 333–343.
23. M. Tabuchi, M. Matsui, T. Watanabe, H. Hongo, K. Kubo and F. Abe: *Mater. Sci. Res. Int.*, 2003, **9**, (1), 23–28.
24. A. W. Marshall, Z. Zhang and G. B. Holloway: Proc. 5th Int. Conf. on 'Welding and repair technology for power plants', Point Clear, AL, USA, June 2002, Electric Power Research Institute.
25. E. L. Bergquist: *Svetsaren*, 1999, **54**, (1–2), 22–25.
26. S. K. Albert, M. Tabuchi, H. Hongo, T. Watanabe, K. Kubo and M. Matsui: *Sci. Technol. Weld. Join.*, 2005, **10**, (2), 149–157.
27. S. K. Albert, M. Matsui, T. Watanabe, H. Hongo, K. Kubo and M. Tabuchi: *ISIJ Int.*, 2002, **42**, (12), 1497–1504.
28. S. K. Albert, M. Matsui, T. Watanabe, H. Hongo, K. Kubo and M. Tabuchi: *Int. J. Press. Vess. Pip.*, 2003, **80**, 405–413.
29. S. L. Mannan and K. Laha: *Trans. Ind. Inst. Met.*, 1996, **49**, (4), 303–320.
30. S. K. Albert, M. Matsui, H. Hongo, T. Watanabe, K. Kubo and M. Tabuchi: *Int. J. Press. Vess. Pip.*, 2004, **81**, 221–234.
31. M. Tabuchi, T. Watanabe, K. Kubo, J. Kinugawa and F. Abe: *Key Eng. Mater.*, 2000, **171–174**, 521–528.
32. T. Kojima, K. Hayashi and Y. Kajita: *ISIJ Int.*, 1995, **35**, (10), 1284–1290.
33. K. Shinozaki, D. Li, H. Kuroki, H. Harada and K. Ohishi: *ISIJ Int.*, 2002, **42**, (12), 1578–1584.
34. R. Wu, R. Sandstrom and F. Seitisleam: *J. Eng. Mater. Technol.*, 2004, **126**, (1), 87–94.
35. J. A. Francis, W. Mazur and H. K. D. H. Bhadeshia: *ISIJ Int.*, 2004, **44**, (11), 1966–1968.
36. J. A. Francis, W. Mazur and H. K. D. H. Bhadeshia: Proc. 7th Int. Conf. on 'Trends in welding research', Pine Mountain, GA, USA, May 2005, ASM International.
37. F. Brun, T. Yoshida, J. D. Robson, V. Narayan, H. K. D. H. Bhadeshia and D. J. C. Mackay: *Mater. Sci. Technol.*, 1999, **15**, (5), 547–554.
38. D. Li, K. Shinozaki, H. Harada and K. Ohishi: *Metall. Mater. Trans. A*, 2005, **36A**, (1), 107–115.
39. D. Li and K. Shinozaki: *Sci. Technol. Weld. Join.*, 2005, **10**, (5), 544–549.
40. P. Hofer, H. Cerjak and P. Warbichler: *Mater. Sci. Technol.*, 2000, **16**, (10), 1221–1225.
41. F. Abe: *Metall. Mater. Trans. A*, 2005, **36A**, (2), 321–332.
42. H. Hirata and K. Ogawa: *Weld. Int.*, 2005, **19**, (2), 109–117.
43. H. Hirata and K. Ogawa: *Weld. Int.*, 2005, **19**, (2), 118–124.
44. Y. Otoguro, M. Matsubara, I. Itoh and T. Nakazawa: *Nucl. Eng. Design*, 2000, **196**, (1), 51–61.
45. T. Watanabe, M. Yamazaki, H. Hongo, M. Tabuchi and T. Tanabe: *Int. J. Press. Vess. Pip.*, 2004, **81**, 279–284.
46. P. Dong: *Sci. Technol. Weld. Join.*, 2005, **10**, (4), 389–398.
47. P. Dong: *J. Press. Vess. Technol. Trans. ASME*, 2001, **123**, (2), 207–213.
48. D. J. Smith, P. J. Bouchard and D. George: *J. Strain Anal.*, 2000, **35**, (4), 287–305.
49. A. H. Yaghi, T. H. Hyde, A. A. Becker, J. A. Williams and W. Sun: *J. Mater. Process. Technol.*, 2005, **167**, 480–487.

50. D. Li, K. Shinozaki and H. Kuroki: *Mater. Sci. Technol.*, 2003, **19**, (9), 1253–1260.
51. S. T. Kimmins and D. J. Smith: *J. Strain Anal.*, 1998, **33**, (3), 195–206.
52. I. J. Perrin and D. R. Hayhurst: *Int. J. Press. Vess. Pip.*, 1999, **76**, 599–617.
53. D. J. Smith, N. S. Walker and S. T. Kimmins: *Int. J. Press. Vess. Pip.*, 2003, **80**, 617–627.